Contents

Introduction **2**

1 Theoretical Background (15 pgs) **5**

Mesoscopic model **6**

1.1 Gross Pitaevskii model 6

1.2 Quantum vortex 7

1.3 Vortex filament model 8

1.4 Vortex dynamics 9

1.5 Kelvin waves 11

Macroscopic model **12**

1.6 Hydrodynamics of two-fluid 12

1.7 Oscillatory motion in superfluid 13

1.8 Quantum turbulence 14

1.9 Second sound 14

Introduction (3 pgs)

The liquid state of ^{4}He exists in two phases:

- Helium I - a high temperature phase ($2.17\,\mathrm{K} < T < 4.2\,\mathrm{K}$)
- Helium II - a low temperature phase ($T < 2.17\,\mathrm{K}$)

These two phases are connected with the *lambda transition*, which occurs at the critical temperature $T_\lambda = 2.17\,\mathrm{K}$ at saturated vapour pressure. Helium I is a classical fluid described by ordinary Navier-Stokes (N-S) equations, whereas Helium II indicates the Bose-Einstein condensate (BEC) in much more way.

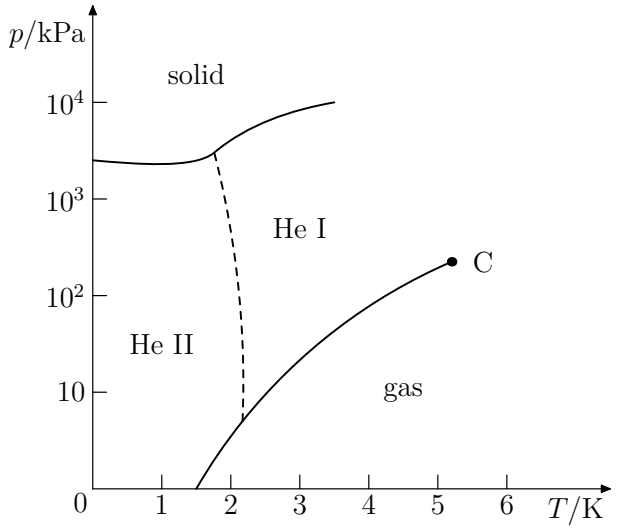

Figure 1: Pressure-Temperature diagram of Helium

A simple, phenomenological model of the Helium II motion was proposed by Tisza and Landau - the *two-fluid theory*. Within this model, Helium II is depicted as a mixture of two fluid components, able to penetrate each other:

- normal component - density ρ_n, velocity field $\mathbf{v}_n$, ordinary viscous N-S equation of motion, carrying entropy and thermal excitations represented by *phonons* and *rotons*
- superfluid component - density ρ_s, velocity field $\mathbf{v}_s$, modified Euler equation (without viscosity) of motion by quantum terms, no entropy, represented by macroscopic wave function

The total density of Helium II sums up to $\rho = \rho_n + \rho_s$ and the relative proportion of normal/superfluid component is determined by the temperature. Near $T \to 0$ Helium II becomes entirely superfluid $\rho_s/\rho \to 1$. The temperature dependence of this ratio is pretty

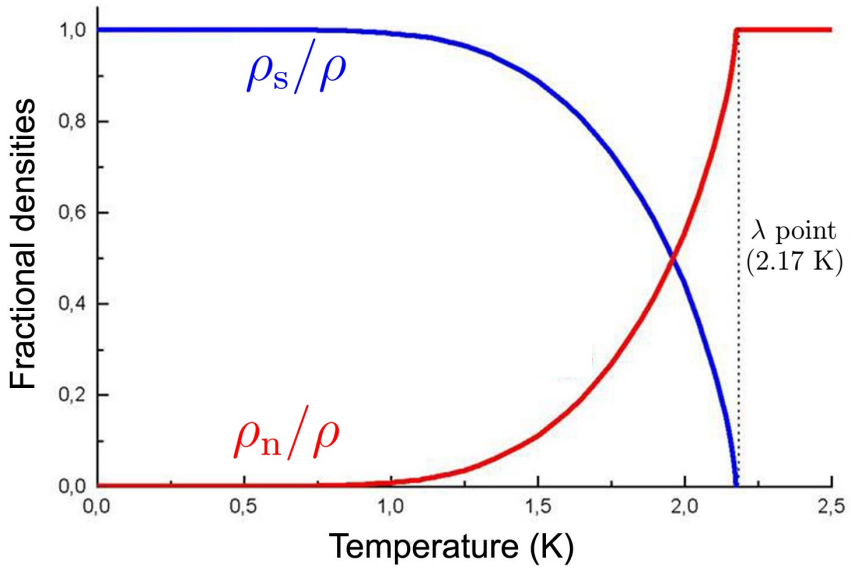

Figure 2: Temperature dependence of density proportions

nonlinear. For example, the ratio ρ_n/ρ drops from 100% at 2.17 K to 50% at 1.95 K, to $< 5\%$ at 1.3 K, and is effectively negligible under 1 K.

The two-fluid model explains many observed phenomena - among others we pick *second sound* and *thermal counterflow* due to their importance in the study pf turbulence.

Second sound: Ordinary sound (the wave of density ρ and pressure P) in Helium II is called *first sound*. In such process, temperature T and entropy S is conserved and $\mathbf{v}_n$ and $\mathbf{v}_s$ oscillate in phase with each others. On the contrary, a second sound is an antiphase oscillation of $\mathbf{v}_n$ and $\mathbf{v}_s$, causing the oscillation of T and S and reamining ρ and P constant. In this work, this phenomena is used for detection of quantized vortices, which naturally appear within Helium II.

Thermal counterflow: Helium II is able to transfer heat in a special way. Let's consider a closed channel filled with Helium II and a dissipating resistor localised at one end of the channel. In normal fluid, the heat is transferred away from the resistor by conduction mechanism. However, in Helium II the heat is carried away only by the normal component. To conserve the total mass flux, some superfluid fluid flow toward the resistor. In this way, a counterflow is generated. If the counterflow is strong enough, the superfluid turbulence is generated.

It arises from the quantum nature of superfluid, that such fluid cannot perform any rotation. It is called then *irrotational*. However, when Helium II rotates or moves faster than a critical velocity, the circulation is *quantized* and so-called *quantized vortices* are created, which makes the hydrodynamics of Helium II particularly interesting. The vortex nucleation process is still a subject of many current investigations. Superfluid vortex lines can be spatially organized (laminar flows) or completely disorganized (turbulent flows).

It has only recently been relized that helium II is an attractive candidate for investigating classical turbulence problems. Quantum turbulence (QT) can be achieved in many tradi-

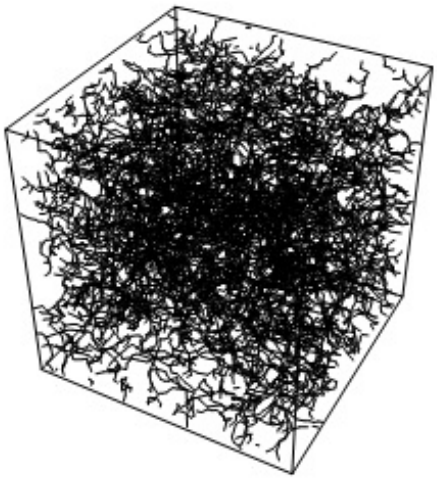

Figure 3: Small simulation cube of tangle of quantum vortices

tional ways - driving a mass flow, spinning discs, oscillating grids and forks, ultrasound, jets. Considering all these methods together, the general trend is that the slow, laminar flow of Helium II (with or without vortices) tends to be rather different from the classical fluid flow. In case of fast motion, the turbulent Helium II seems to behave similar to classical turbulent flow.
To characterize the turbulence we use the dimensionless Reynolds number. Examples of the observed classical features of Helium II QT (regardless on temperature) were found during experiments with flow strength of $\mathrm{Re} \approx 10^6$ (pressure drops), of $\mathrm{Re} \approx 10^5$ (sphere drag crisis), of $\mathrm{Re} \approx 4 \times 10^4$ (whole fluid vorticity) and of $\mathrm{Re} \approx 4 \times 10^3$ (structures of turbulence).

In classical fluid dynamics (solutions of motion equations), the useful tool for understanding the geometry and dynamics of flow is *vortex filament model*. With the rapid development of available computational power, large simulations have become the methods of choice for calculating the motion of fluids. In superfluids like Helium II, due to the quantization of circulation, vorticity can only exist within vortex filaments with a certain core size, which makes the model a way more applicable than in fields of classical fluids.

Motivations and Goals

Motivations:

- no 1
- no 2
- no 2

Goals:

- no 1
- no 2
- no 2

Motivations: investigate critical velocities and vortex density, create numeric model

Goals: measure hydrodynamic profiles for more temperatures with oscillating object, transition from CT to QT, investifate numerically vortex rings

1. Theoretical Background (15 pgs)

The theoretical part of this Thesis is composed of two chapters:

1. Mesoscopic view - theoretically cover London's theory, creation and numerical modelling of quantum vortex, vortex dynamics.

3. Macroscopic view - hydrodynamics of two-fluid model, oscillatory motion in such fluid, creation of QT, existence and usage of second sound

The aim of this part of thesis is to introduce the basic properties of quantized vortex lines in Helium II and summarize the main experimental observations of superfluid turbulence. Then there is discussed the theoretical methods used to study quantized vorticity, quantum turbulence and the results obtained using such methods.

Mesoscopic view

One of the most useful ways of describing superfluid helium at $T = 0$ starts with nonlinear Schrodinger equation (NLSE) for the one-particle wave function ψ. Since superfluid helium is a strongly correlated system dominated by collective effects, this imperfect Bose condensate is described by Gross-Pitaevskii equation.

1.1 Gross Pitaevskii model

In terms of single-particle wavefunction $\psi(\mathbf{r}, t)$:

$$i\hbar\frac{\partial\psi}{\partial t} = -\frac{\hbar^2}{2m}\nabla^2\psi + \psi\int|\psi(\mathbf{r}', t)|^2 V(|\mathbf{r} - \mathbf{r}'|)\mathrm{d}\mathbf{r}', \tag{1.1}$$

where $V(|\mathbf{r} - \mathbf{r}'|)$ is the potential of two-body interaction between bosons. The normalization is set as $\int|\psi|^2\mathrm{d}\mathbf{r} = N$, where N is number of bosons. By replacing potential with repulsive δ-function of strength V_0 one obtains:

$$i\hbar\frac{\partial\Psi}{\partial t} = -\frac{\hbar^2}{2m}\nabla^2\Psi - m\varepsilon\Psi + V_0|\Psi|^2\Psi, \tag{1.2}$$

where ε is the energy per unit mass and $\Psi = Ae^{i\Phi}$ is a macroscopic wave function of condensate. In this way one can define the condensate's density $\rho_{BEC} = m\Psi\Psi^* = mA^2$ and velocity $\mathbf{v}_{BEC} = (\hbar/m)\nabla\Psi$. Note that equation (1.2) is equivalent to a continuity equation and an modified Euler equation (by the so called quantum pressure term).

Even the superfluid is irrotational $\omega = \nabla \times \mathbf{v}_{BEC} = \mathbf{0}$, the NLSE has a vortex-like solution: $\mathbf{v}_s = \Gamma/2\pi r\,\mathbf{e}_\theta$, where θ is the azimuthal angle and $\Gamma = 9.97 \times 10^{-4}\,\mathrm{cm}^2\cdot\mathrm{s}^{-1}$ is the *quantum of circulation*, obtained from:

$$\Gamma = \oint_{\mathcal{C}}\mathbf{v}_{BEC}\cdot\,\mathrm{d}\boldsymbol{\ell} = \frac{h}{m} \tag{1.3}$$

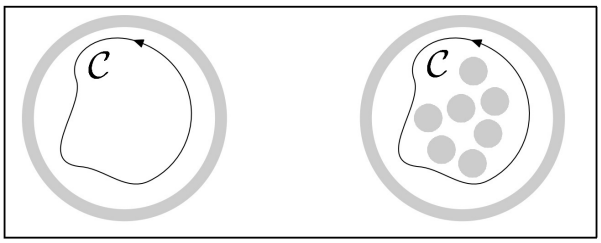

Figure 1.1: topological singularities within superfluid

1.2 Quantum vortex

Superfluid vortex lines appear when helium II moves faster than a critical velocity. Such *nucleation* is the subject of many investigations and is introduced widely later in this work.

The simplest way to create quantum vortices is to rotate cylinder with superfluid Helium II with high enough angular velocity Ω. Created vortex lines form an ordered array of density $L = 2\Omega/\Gamma$, all aligned along the axis of rotation. *Vortex line density* L can be also interpreted as a total vortex length in an unit volume.

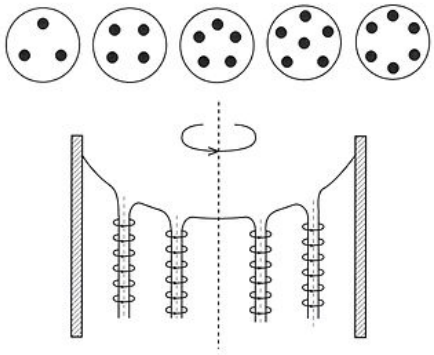

Figure 1.2: Array of quantized vortices in a rotating container

The key properties of Onsager-Feynman vortex are the quantized circulation Γ, superfluid rotational velocity field $\mathbf{v}_s = \Gamma/2\pi r\,\mathbf{e}_\theta$ and the *vortex core parameter* a_0. The core size a_0 can be estimated by substituting $\mathbf{v}_s$ back into (1.2) and solving differential equation for ρ_s. One finds that ρ_s tends to the value $m^2\varepsilon/V_0$ for $r \to \infty$ and to zero density for $r \to 0$. The characteristic distance over which Ψ collapses (superfluid density ρ_s drops from bulk value to zero) is $a_0 \approx 10^{-10}\,\mathrm{m} = 1\,\text{Å}$.

From this, there is a conclusion that the vortex is hollow at its core and therefore, the topological defect occurs. Although, it must be noted that real Helium II is a dense fluid, not weakly interacting Bose gas described by NLSE.

Taking a as core radius and b as characteristic distance between two vortices, one can derive the unit length energy for vortex line:

$$\varepsilon_n = \int_{S_a}^{S_b} \varepsilon_{kin}\,\mathrm{d}S = \frac{\pi\hbar^2\rho_\mathrm{s}\ln(b/a)}{m^2}\,n^2 \tag{1.4}$$

Since $E_\mathrm{vortex} \sim n^2$, an N quantum vortices contains more energy than N single quantum vortices, and it is generally assumed that only single quantum vortices are commonly observed.

Clearly, vortex lines don't have to be aligned in general. In most cases , the superfluid flow is strongly chaotic, better known as *quantum turbulence*. This topic is covered in more detail later in this work.

1.3 Vortex filament model

The vortex line can be represented as a curve via positional vector $\mathbf{s} = \mathbf{s}(\xi, t)$ in three-dimensional space. Here, ξ is arclength along the vortex line. Next we label $\mathbf{s}'$ as $\mathrm{d}\mathbf{s}/\mathrm{d}\xi$ and $\mathbf{s}''$ as $\mathrm{d}\mathbf{s}'/\mathrm{d}\xi$. Within our context, $\mathbf{s}'$ is a tangent vector and $|\mathbf{s}''|$ is a local curvature R^{-1} at a given point. The triad of vectors $\mathbf{s}$, $\mathbf{s}'$, $\mathbf{s}' \times \mathbf{s}''$ are perpendicular to each other and point along the tangent, normal and binormal respectively:

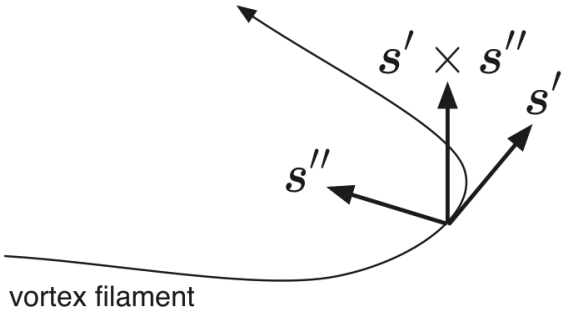

Figure 1.3: Schematic of the vortex filament and the triad vectors

We suppose that the superfluid component is incompressible $\nabla \cdot \mathbf{v}_s = 0$. Moreover, superfluid vorticity ω_s is localized only at positions of vortex filaments:

$$\omega_s(\mathbf{r}, t) = \nabla \times \mathbf{v}_s = \Gamma \int_{\mathcal{L}} \mathrm{d}\xi \, \mathbf{s}'(\xi, t) \delta(\mathbf{r} - \mathbf{s}(\xi, t)) \,, \tag{1.5}$$

where the integral path $\mathcal{L}$ represents curves along all vortex filaments. From incompressibility and (1.5), we obtain Biot-Savart law for the superfluid velocity:

$$\mathbf{v}_s(\mathbf{r}) = \frac{\Gamma}{4\pi} \int_{\mathcal{L}} \frac{(\mathbf{r}' - \mathbf{r}) \times \mathrm{d}\mathbf{r}'}{|\mathbf{r}' - \mathbf{r}|^3} \tag{1.6}$$

This law determines the superfluid velocity field via the arrangement of the vortex filaments. Now we define the *self-induced* velocity $\mathbf{v}_i$, describing the motion which a vortex line induces onto itself due to its own curvature:

$$\mathbf{v}_i(\mathbf{s}) = \frac{\Gamma}{4\pi} \int_{\mathcal{L}} \frac{(\mathbf{r}' - \mathbf{s}) \times \mathrm{d}\mathbf{r}'}{|\mathbf{r}' - \mathbf{s}|^3} \tag{1.7}$$

Although, this integral diverges as $\mathbf{r}' \to \mathbf{s}$ because the core structure of the quantized vortex was neglected. We avoid this divergence by splitting the integral into two parts - direct neighborhood of the point $\mathbf{s}$ (local part) and the rest part $\mathcal{L}'$ (nonlocal part). The Taylor expansion of the local part leads to finite result and thus:

$$\mathbf{v}_i(\mathbf{s}) = \mathbf{v}_{\mathrm{s,local}} + \mathbf{v}_{\mathrm{s,nonlocal}} \approx \beta \mathbf{s}' \times \mathbf{s}'' + \frac{\Gamma}{4\pi} \int_{\mathcal{L}'} \frac{(\mathbf{r}' - \mathbf{s}) \times \mathrm{d}\mathbf{r}'}{|\mathbf{r}' - \mathbf{s}|^3} \,, \tag{1.8}$$

where $\beta = (\Gamma/4\pi)\ln(1/|\mathbf{s}'|a_0)$. This process is called Local Induction Approximation (LIA). Numerical study of Adachi et al. showed that the nonlocal term plays an important role even for homogeneous quantum turbulence.

Since there could be also external flow source of superfluid component, we define the total superfluid velocity, in laboratory frame, as:

$$\mathbf{v}_{s,tot} = \mathbf{v}_{s,ext} + \mathbf{v}_i \tag{1.9}$$

1.4 Vortex dynamics

To determine the equation of motion of $\mathbf{s}$ we must recognize the forces acting upon the line - the magnus force $\mathbf{f}_M$ and (at temperature $T > 0$), the drag force $\mathbf{f}_D$ (both are per unit length).

The magnus force always arises when a rotating body moves in a flow - the rotation creates an increased velocity on one side and decreased velocity on the other one. This causes a pressure difference, which in our case of moving vortex line with circulation quantum Γ, exerts a force:

$$\mathbf{f}_M = \rho_s \Gamma \mathbf{s}' \times (\dot{\mathbf{s}} - \mathbf{v}_{s,tot}), \tag{1.10}$$

where $\mathbf{dots} = \mathrm{d}\mathbf{s}/\mathbf{d}t$ is the velocity of the line filament in the laboratory frame.

The drag force $\mathbf{f}_D$ arises from the *mutual friction*, the interaction between the normal component and superfluid component. According to Vinen and Hall foundings, the normal fluid flowing with velocity $\mathbf{v}_n$ past a vortex core exerts a frictional force $\mathbf{f}_D$ on the superfluid, given by:

$$\mathbf{f}_D = -\alpha(T)\rho_s\Gamma\mathbf{s}' \times [\mathbf{s}' \times (\mathbf{v}_n - \mathbf{v}_{s,tot})] - \alpha'(T)\Gamma\mathbf{s}' \times (\mathbf{v}_n - \mathbf{v}_{s,tot}) \tag{1.11}$$

The temperature dependent dimensionless parameters $\alpha(T)$ and $\alpha'(T)$ are written in terms of *mutual friction parameters* B and B', which are known from experiments by Samuels and Donnelly:

$$\alpha(T) = \frac{\rho_n B(T)}{2\rho} \qquad \alpha'(T) = \frac{\rho_n B'(T)}{2\rho} \tag{1.12}$$

The precise calculation of the mutual friction parameters over the entire temperature range is still an open problem. Although, we already know that friction arises from the scattering process of rotons in the area of high temperatures.

Since the mass of vortex core is usually neglected, the two forces $\mathbf{f}_M$ and $\mathbf{f}_D$ sum up into zero: $\mathbf{f}_M + \mathbf{f}_D = \mathbf{0}$. Hence, solving for $\mathrm{d}\mathbf{s}/\mathrm{d}t$, we obtain the Schwarz's equation:

$$\dot{s} = \mathbf{v}_s + \mathbf{v}_i + \alpha \mathbf{s}' \times (\mathbf{v}_{ns} - \mathbf{v}_i) - \alpha' \mathbf{s}' \times [\mathbf{s}' \times (\mathbf{v}_{ns} - \mathbf{v}_i)] \,, \tag{1.13}$$

where $\mathbf{v}_{ns} = \mathbf{v}_n - \mathbf{v}_s$ is the difference between the average velocity of normal fluid and the applied superfluid velocity.

On the basis of Schwarz's equation there can be developed an algorithm to numerically simulate vortex time evolution of an arbitrary configuration. More on this is written later in Simulation part of thesis.

Quantized vortex rings

A special case of vortex line configuration is a freely moving vortex ring. Such rings are usually created as a result of multi-vortex interconnection and have limited life expectancy. The exact expressions derived by classical hydrodynamics for the energy E_{ring} and center velocity v_{ring}, moving in a Helium II of density ρ and having a radius R much greater than its core radius $R >> a_0$, are

$$E_{\text{ring}} = \frac{1}{2}\Gamma^2 \rho R \Big(\ln(8R/a_0) - 2 + c \Big) \tag{1.14}$$

$$v_{\text{ring}} = \frac{\Gamma}{4\pi R} \Big(\ln(8R/a_0) - 1 + c \Big) \,, \tag{1.15}$$

where c is a constant based on inner structure of the vortex. Since we work with hollow core, we use $c = 0$. Note that (1.14) and (1.15) depend on a_0 only logarithmically. The behavior of the vortex ring is thus quite insensitive to the exact value of a_0 (expected to be of the order of atomic dimension).

!!TODO!! L ife expectancy

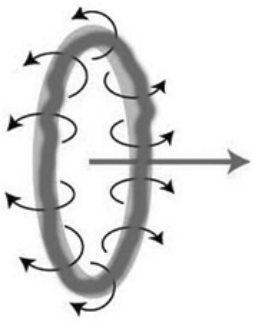

Figure 1.4: Depiction of quantized vortex ring motion

1.5 Kelvin waves

!!TODO!!

Macroscopic view

1.6 Hydrodynamics of two-fluid

- Landau's assumptions
- two densities, velocities (+pic)
- updated hydrodynamical equations - HVBK
- dynamical similarity
- Reynolds number

HVBK equations:

$$\frac{\partial \mathbf{v}_n}{\partial t} + (\mathbf{v}_n \cdot \nabla)\mathbf{v}_n = -\frac{1}{\rho}\nabla P - \frac{\rho_s}{\rho_n} S\nabla T + \nu_n \nabla^2 \mathbf{v}_n + \mathbf{F}_{ns}\,, \tag{1.16}$$

$$\frac{\partial \mathbf{v}_s}{\partial t} + (\mathbf{v}_s \cdot \nabla)\mathbf{v}_s = -\frac{1}{\rho}\nabla P + S\nabla T + \mathbf{T} - \frac{\rho_n}{\rho}\mathbf{F}_{ns}\,, \tag{1.17}$$

, where we have defined:

$$\boldsymbol{\Omega}_s = \nabla \times \mathbf{v}_s\,, \tag{1.18}$$

$$\mathbf{F} = \frac{B}{2}\hat{\boldsymbol{\Omega}} \times [\hat{\boldsymbol{\Omega}}_s \times (\mathbf{v}_n - \mathbf{v}_s - \nu_s \nabla \times \hat{\boldsymbol{\Omega}})] + \frac{B'}{2}\boldsymbol{\Omega}_s \times (\mathbf{v}_n - \mathbf{v}_s - \nu_s \nabla \times \hat{\boldsymbol{\Omega}}_s)\,, \tag{1.19}$$

$$\hat{\boldsymbol{\Omega}}_s = \boldsymbol{\Omega}_s / |\boldsymbol{\Omega}_s|\,, \tag{1.20}$$

$$\mathbf{T} = -\nu_s \boldsymbol{\Omega}_s \times (\nabla \times \hat{\boldsymbol{\Omega}}_s) \tag{1.21}$$

$$\nu_s = \frac{\Gamma}{4\pi}\log(b_0/a_0) \tag{1.22}$$

Drag coeff:

$$C_D \propto v^\alpha, \qquad \text{where} \begin{cases} \alpha = -1 & \text{for Re} \in (0-10) \\ \alpha = 0 & \text{for Re} \in (10^3 - 10^5) \end{cases}.$$

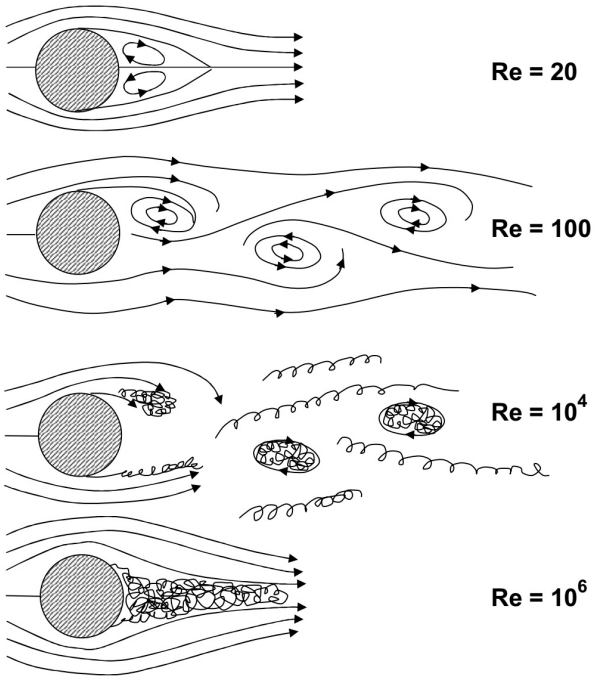

Figure 1.5: transition from laminar to turbulent flow

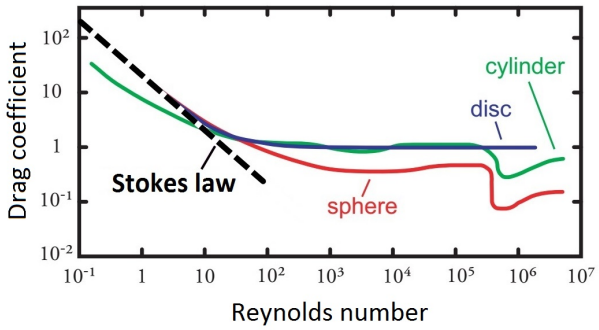

Figure 1.6: drag coeffs of different objects

1.7 Oscillatory motion in superfluid

- penetration depth
- Re for oscillations
- defining depth and Re separately for normal and superfluid components

Attenuated wave:

$$\mathbf{v} \propto e^{-|\mathbf{r}|/\delta} \hat{\mathbf{e}}_{\mathbf{r}}(\omega, t)\,, \tag{1.23}$$

Penetration depth:

$$\delta = \sqrt{\frac{2\nu}{\omega}}\,. \tag{1.24}$$

Oscillatory Reynolds number:

$$\mathrm{Re}_\delta = \frac{v_0\delta}{\nu} = \frac{v_0}{\sqrt{\nu\pi f}}\,. \tag{1.25}$$

Depth and Re for normal component:

$$\delta_\mathrm{n} = \sqrt{\frac{2\eta}{\rho_\mathrm{n}\omega}}\,, \qquad \mathrm{Re}_\mathrm{n} = \frac{v_0\delta_\mathrm{n}\rho_\mathrm{n}}{\eta}\,. \tag{1.26}$$

1.8 Quantum turbulence

- critical velocity according to landau
- critical velocity scaling in oscillatory case
- T dependence of critical velocities (Bc. results)

Critical velocity scaling:

$$v_\mathrm{crit} \propto \sqrt{\omega} \tag{1.27}$$

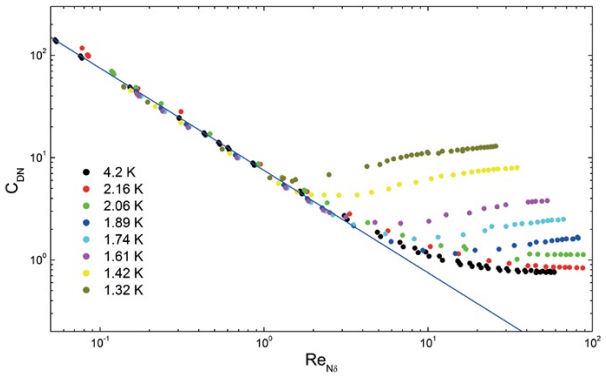

Figure 1.7: drag coeffs vs Reynolds number of normal component

1.9 Second sound

- what it is

- velocity of second sound
- attenuation
- vortex line density estimate

$$\mathbf{v}_{\mathrm{ns}} \propto e^{-\alpha z}\hat{\mathbf{e}}_{\mathbf{r}}(\mathbf{k},\mathbf{r},\omega,t)\,, \tag{1.28}$$

$$\alpha = \frac{B\kappa L}{6c_2}\,. \tag{1.29}$$

First and second sounds:

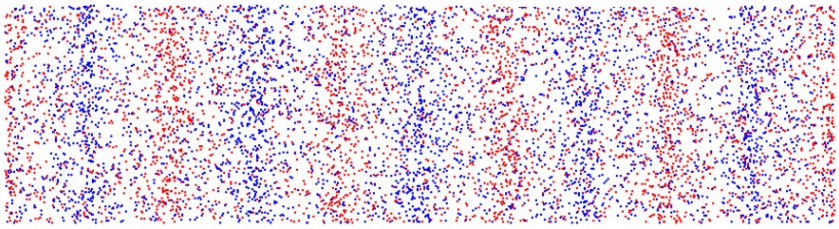

Figure 1.8: first mode of second sound

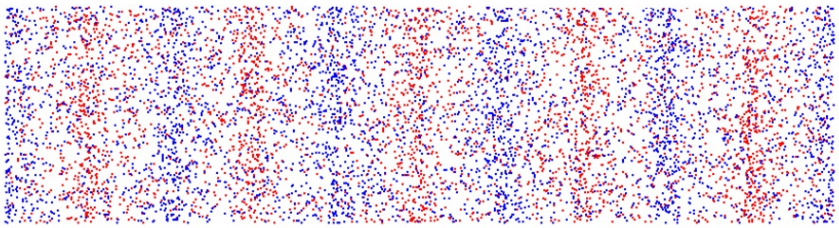

Figure 1.9: second mode of second sound

Velocity of second sound with temperature:

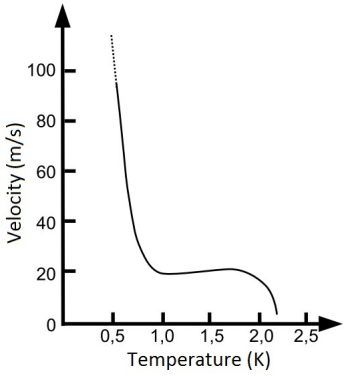

Figure 1.10: velocity of ss with temperature

Vortex line density:

$$L = \frac{6\pi\Delta f_0}{B\kappa}\left(\frac{A_0}{A} - 1\right), \tag{1.30}$$